- ¹ Xinxin Peng
- ² Xiaojun Wang
- ³ Huijuan Li
- ⁴ Fang Cao

Sensorless Control of PMSM Based on Fuzzy Integral Terminal Sliding Mode Observer



Abstract: - To address the challenges of low estimation accuracy and strong chattering in traditional sliding mode observer (SMO) for permanent magnet synchronous motors (PMSM), a fuzzy integral terminal sliding mode observer (FITSMO) is proposed. First, based on the analysis of nonlinear sliding mode surface theory, an integral-type terminal sliding mode surface is constructed, which enables the current observation error to converge to zero within a finite time, effectively reducing chattering phenomena and enhancing the accuracy of the system's observation. Then, the fuzzy logic controller (FLC) is introduced to combine the sliding mode gain and fuzzy control by designing the fuzzy rule base and the membership function, so that the sliding mode gain is dynamically adjusted according to the actual operating conditions. Both simulation and experimental results demonstrate that the proposed algorithm can enhance the speed and accuracy of position observation for the sliding mode observer.

Keywords: PMSM; SMO; Sensorless drive; FLC; FITSMO.

I. INTRODUCTION

In recent years, PMSM have developed rapidly due to their advantages such as compact size, high power factor, low rotational inertia, and energy-efficient performance. These characteristics have led to their widespread application in aerospace, electric vehicles, intelligent robotics, industrial production, and other fields [1]-[6]. To achieve precise control of PMSM, accurate rotor position information is a prerequisite for vector control. Traditionally, rotor position is obtained by installing mechanical position sensors on the motor shaft. However, this approach increases the cost and complexity of the system, and also risks sensor performance degradation or failure in harsh environments. Therefore, research on sensorless control [7] systems for PMSM holds significant practical importance.

Sensorless control technology uses electrical signals detected in the motor windings to estimate the rotor position, such as stator voltage and current, and uses control algorithms to estimate the rotor speed and position. In recent years, research on PMSM sensorless control systems has made substantial progress, with numerous scholars worldwide proposing various control methods. Currently, the primary approaches for PMSM sensorless control include: the model reference adaptive system method [8]; the high-frequency signal injection method [9]; neural network-based methods [10]; the extended Kalman filter algorithm [11]; and the sliding mode observer method [12], among others.

The design of sliding mode observer is based on the mathematical model under the stationary coordinate system. By utilizing the two-phase stationary coordinate system current state equations of PMSM, a current sliding mode observer is designed. The sliding mode surface is designed using the current error value obtained by comparing the observed and measured values. By comparing the observer equations with the system state equations, estimates of the back electromotive force (EMF) can be obtained. The reconstructed back EMF inherently contains information about the rotor position and speed. While SMO methods offer advantages such as simple parameter design and strong robustness, traditional SMO suffer from high-frequency chattering, which degrades system estimation accuracy. Therefore, mitigating chattering in sliding mode systems has become a key focus in SMO research. Some researchers have attempted to design higher-order sliding modes to reduce chattering and improve convergence speed. For instance, literature [13] introduced an integral-type nonsingular terminal sliding mode surface to avoid phase lag in back EMF estimation caused by low pass filter (LPF). However, this approach involves complex parameter tuning and implementation challenges. Literature [14] employed a supertwisting SMO to enhance disturbance rejection, but its high computational burden limits practical engineering applications. Literature [15] and [16] combined the first-order norm and switching function with traditional reaching laws to propose an adaptive exponential reaching law. This method adaptively adjusts the system's convergence speed based on changes in the sliding surface and system states, thereby reducing high-frequency chattering in back EMF estimation. While, parameter tuning complexity persists in such adaptive exponential reaching laws. The discontinuous sign function used as the switching function is another major cause of high-frequency chattering in SMO. Literature [17] and

^{2*}Corresponding author: Xiaojun Wang, E-mail: 997601814@qq.com ^{1,2,3,4}, School of Electrical and Electronics Engineering, Chongqing University of Technology Copyright © JES 2025 on-line: journal.esrgroups.org

[18] improves upon the traditional SMO by using a saturation function instead of a sign function. This method effectively eliminates jitter vibration during high-speed motor operation to a certain extent and achieves accurate estimation of the rotor's position and speed. However, this approach degrades convergence performance and robustness. To expand the speed range applicable to SMO, literature [19] proposed adaptively modifying the sliding mode gain using a simple mathematical function. This method is only applicable for gain adjustment under fixed-speed operating conditions. With the advancement of microprocessor computational capabilities, researchers have integrated advanced intelligent control algorithms, such as fuzzy logic and neural networks, into sliding mode control systems to optimize system performance [20]. Literature [21] describes the construction of a fuzzy controller for achieving a variable sliding mode gain design, using the speed error and the rate of change of the motor as the input variables. However, this approach only detects speed changes and results in poor dynamic performance.

Based on the above control strategy, this paper proposes a novel integral terminal sliding mode control algorithm, which can effectively suppress chattering. Secondly, a fuzzy control method is adopted for the sliding mode switching gain of the sliding mode control, enabling it to change with the distance from the sliding mode surface. As verified by simulation and experimental results, the method used in this paper improves the accuracy of rotor position and speed observation.

II. CONVENTIONAL SMO

In the two-phase stationary $\alpha\beta$ coordinate system, the voltage model of the motor is:

$$\begin{bmatrix} u_{\alpha} \\ u_{\beta} \end{bmatrix} = \begin{bmatrix} R_s + \Delta L_d & \omega_e (L_d - L_q) \\ -\omega_e (L_d - L_q) & R_s + \Delta L_q \end{bmatrix} \begin{bmatrix} i_{\alpha} \\ i_{\beta} \end{bmatrix} + \begin{bmatrix} E_{\alpha} \\ E_{\beta} \end{bmatrix}$$
(1)

$$\begin{bmatrix} E_{\alpha} \\ E_{\beta} \end{bmatrix} = \left[(L_d - L_q)(\omega_e i_d - \Delta i_q) + \omega_e \psi_f \right] \begin{bmatrix} -\sin \theta_e \\ \cos \theta_e \end{bmatrix}$$
 (2)

Where L_d and L_q is the stator inductance; ω_e is the electrical angular velocity; ψ_f is the permanent magnet flux linkage; θ_e is the rotor position angle; Δ is the differential operator; $\begin{bmatrix} u_{\alpha} & u_{\beta} \end{bmatrix}^T$ are the stator voltages; $\begin{bmatrix} i_{\alpha} & i_{\beta} \end{bmatrix}^T$ are the stator current; $\begin{bmatrix} E_{\alpha} & E_{\beta} \end{bmatrix}^T$ are the extended back electromotive force.

For the surface-mounted three-phase PMSM, rewrite the voltage equation (1) in the form of an equation of state for current.:

$$\frac{d}{dt} \begin{bmatrix} i_{\alpha} \\ i_{\beta} \end{bmatrix} = -\frac{R}{L_{s}} \begin{bmatrix} i_{\alpha} \\ i_{\beta} \end{bmatrix} + \frac{1}{L_{s}} \begin{bmatrix} u_{\alpha} \\ u_{\beta} \end{bmatrix} - \frac{1}{L_{s}} \begin{bmatrix} E_{\alpha} \\ E_{\beta} \end{bmatrix}$$
 (3)

To obtain an estimate of the extended back electromotive force, a conventional SMO is usually designed as follows:

$$\frac{d}{dt} \begin{bmatrix} \hat{i}_{\alpha} \\ \hat{i}_{\beta} \end{bmatrix} = -\frac{R}{L_s} \begin{bmatrix} \hat{i}_{\alpha} \\ \hat{i}_{\beta} \end{bmatrix} + \frac{1}{L_s} \begin{bmatrix} u_{\alpha} \\ u_{\beta} \end{bmatrix} - \frac{1}{L_s} \begin{bmatrix} v_{\alpha} \\ v_{\beta} \end{bmatrix}$$
(4)

Where: \hat{i}_{α} and \hat{i}_{β} are the observed values of the stator current; u_{α} and u_{β} are the control inputs of the observer. By subtracting equation (4) from equation (3), the error equation of the stator current can be obtained as follows:

$$\frac{d}{dt} \begin{bmatrix} \tilde{i}_{\alpha} \\ \tilde{i}_{\beta} \end{bmatrix} = -\frac{R}{L_{s}} \begin{bmatrix} \tilde{i}_{\alpha} \\ \tilde{i}_{\beta} \end{bmatrix} + \frac{1}{L_{s}} \begin{bmatrix} E_{\alpha} - v_{\alpha} \\ E_{\beta} - v_{\beta} \end{bmatrix}$$
 (5)

Where: $\tilde{i}_{\alpha} = \hat{i}_{\alpha} - i_{\alpha}$ and $\tilde{i}_{\beta} = \hat{i}_{\beta} - i_{\beta}$ are the current observation errors. Design the sliding surface function S and the sliding mode control law v as follows:

$$S^{T} = \begin{bmatrix} \tilde{i}_{\alpha} & \tilde{i}_{\beta} \end{bmatrix} = 0 \tag{6}$$

$$\begin{bmatrix} v_{\alpha} \\ v_{\beta} \end{bmatrix} = \begin{bmatrix} k \operatorname{sgn}(\hat{i}_{\alpha} - i_{\alpha}) \\ k \operatorname{sgn}(\hat{i}_{\beta} - i_{\beta}) \end{bmatrix}$$
 (7)

Once the observer state variable has reached the slip mode surface, it will remain there. According to the equivalent control principle of sliding mode control, the control quantity at this time can be regarded as the equivalent control quantity, which can be obtained as follows:

$$\begin{bmatrix} E_{\alpha} \\ E_{\beta} \end{bmatrix} = \begin{bmatrix} v_{\alpha} \\ v_{\beta} \end{bmatrix} = \begin{bmatrix} k \operatorname{sgn}(\tilde{i}_{\alpha}) \\ k \operatorname{sgn}(\tilde{i}_{\beta}) \end{bmatrix}$$
(8)

As can be seen from equation (8), due to the presence of high-frequency switching signals in the extended back electromotive force, this will cause system chattering. To reduce the chattering, the low pass filter is usually introduced for filtering:

$$\hat{E}_{\alpha} = \frac{\omega_{c}}{s + \omega_{c}} v_{\alpha}
\hat{E}_{\beta} = \frac{\omega_{c}}{s + \omega_{c}} v_{\beta}$$
(9)

Where: ω_c is the cutoff angular frequency; \hat{E}_{α} and \hat{E}_{β} are the observed value of back electromotive force. However, the presence of the low pass filter will introduce phase delay, so it is necessary to compensate for its phase angle. At this point, the expressions for the estimated motor speed and position angle are:

$$\hat{\boldsymbol{\Theta}}_{e} = \sqrt{\hat{E}_{\alpha}^{2} + \hat{E}_{\beta}^{2}} / \psi_{f}$$

$$\hat{\boldsymbol{\theta}}_{e} = \arctan\left(\frac{-\hat{E}_{\alpha}}{\hat{E}_{\beta}}\right) + \arctan\left(\frac{\hat{\boldsymbol{\omega}}_{e}}{\boldsymbol{\omega}_{c}}\right)$$
(10)

III. IMPROVED SMO

To improve the observation accuracy and accurately estimate the rotor position and speed of the motor, and at the same time enable the system control state variables to rapidly converge to the sliding surface within a finite time, this paper proposes an integral terminal sliding mode observer (ITSMO), which can effectively reduce system chattering and estimation errors.

A. The integral terminal sliding surface

Taking \tilde{i} as the state variable, the integral terminal sliding surface is designed as follows to achieve rapid convergence of the system state to the equilibrium state within a finite time:

$$s = \tilde{i} + \int_0^t (a\tilde{i} + b \operatorname{sig}^{\varphi}(\tilde{i}) d\tau \tag{11}$$

Where: $a, b > 0, 0 < \varphi < 1$

$$\operatorname{sig}^{\varphi}(x) = |x|^{\varphi} \operatorname{sgn}(x) \tag{12}$$

When the state variable enters the sliding mode, we have $s = \dot{s} = 0$ and

$$\dot{\tilde{i}} + a\tilde{i} + b |\tilde{i}|^{\varphi} \operatorname{sgn}(\tilde{i}) = 0$$
(13)

For any initial state with $\tilde{i}_{(0)} \neq 0$, the state variables will eventually converge to the equilibrium state after a finite time t_s . By solving the differential equation (13), the convergence time of $\tilde{i}_{(t_s)} = 0$ can be obtained as:

$$t_s = \frac{1}{a(1-\varphi)} \ln \frac{a \left| \tilde{i}_{(0)} \right|^{1-\varphi} + b}{b} \tag{14}$$

From equation (13), when the error states are at different distances from the equilibrium point, the linear term $a\tilde{i}$ and the nonlinear term $b |\tilde{i}|^{\varphi} \operatorname{sgn}(\tilde{i})$ play different roles. Therefore, the integral terminal sliding surface proposed in this paper can effectively achieve global and rapid convergence. Moreover, compared with the traditional terminal sliding surface, by introducing the integral term, there is no differential state, and the singularity phenomenon is also avoided.

B. Estimation of the back EMF

To obtain the back electromotive force, we need to design the corresponding control law v, which typically consists of an equivalent control v_{eq} and a switching control v_{sw} . The control law is designed as follows:

$$v = v_{eq} + v_{sw}$$

$$v_{eq} = R_s \tilde{i} - L(a\tilde{i} + b|\tilde{i}|^{\varphi} \operatorname{sgn}(\tilde{i}))$$

$$v_{sw} = -k|s|^{\varphi} \operatorname{sgn}(s) - \eta s$$
(15)

Analyzing equation (15), the equivalent control term v_{eq} can be derived from $\dot{s} = 0$ without considering the back electromotive force. In this control system, the fast power reaching law is combined with the exponential reaching law to obtain the switching control term v_{sw} for robust control against uncertainties and disturbances. The sliding mode control law function can be expressed as:

$$v = R_s \tilde{i} - L(a\tilde{i} + b|\tilde{i}|^{\varphi} \operatorname{sgn}(\tilde{i})) - k|s|^{\varphi} \operatorname{sgn}(s) - \eta s$$
(16)

According to the Lyapunov theorem, if the system satisfies $s\dot{s} < 0$, the system is asymptotically stable, meaning that the system state variables have the advantage of stabilizing in a short time.

IV. FUZZY LOGIC CONTROLLER

To further reduce the chattering problem in sliding mode control, fuzzy logic controller is introduced into the sliding mode control. By using s and \dot{s} as the inputs of the fuzzy controller, fuzzy rules and membership functions are designed to make the sliding mode gain adaptively change, improve the convergence speed under the condition of ensuring stability, and weaken the system chattering. The membership functions for the input and output of the FLC are illustrated in Fig. 1, respectively. And the relevant fuzzy sets are defined as table I.

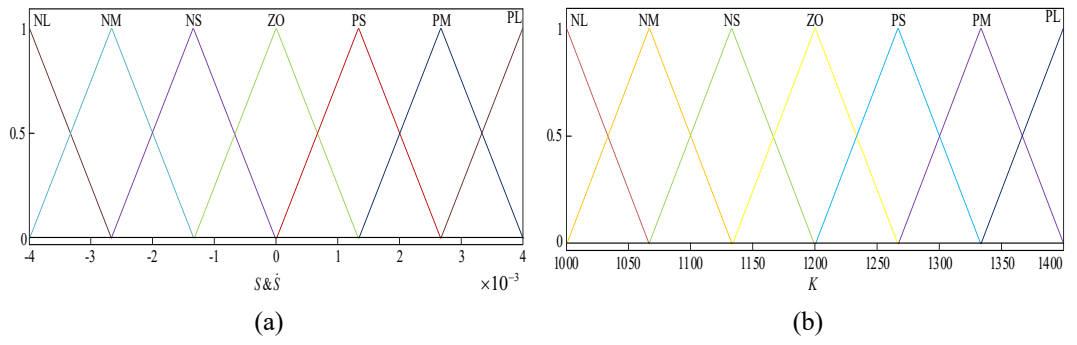


Fig.1. Membership functions for FLC (a) input and (b) output

TABLE I. Fuzzy rules							
s s	NL	NM	NS	ZO	PS	PM	PL
NL	NL	NL	NL	NM	NS	NS	ZO
NM	NL	NM	NM	NM	NS	ZO	ZO
NS	NM	NM	NS	NS	ZO	ZO	PS
ZO	NS	NS	ZO	ZO	ZO	PS	PS
PS	NS	ZO	ZO	PS	PS	PM	PM
PM	ZO	ZO	PS	PM	PM	PM	PL
PL	ZO	PS	PM	PM	PL	PL	PL

Fuzzy rules are designed so that the switching gain of the ITSMO system varies with the distance between the state variables and the sliding surface. When the system state variables are far from the sliding surface, the sliding mode gain is large, and the convergence speed is fast; when the system state variables are close to the sliding surface, the sliding mode gain is small, and the convergence speed is slow, thereby weakening the chattering of the system. Then the principle of fuzzy integral terminal sliding mode observer is shown in Fig. 2.

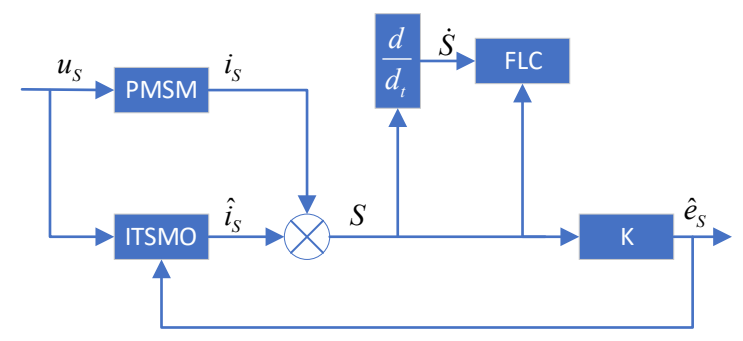


Fig.2. Block diagram of FITSMO

V. SIMULATION AND EXPERIMENTAL VERIFICATION

To analyze the observation performance of the novel FITSMO proposed in this paper, a simulation model is built in Matlab/Simulink to verify its correctness through simulation. A vector control strategy with $i_d = 0$ is adopted to achieve sensorless control of the PMSM. The parameters of the PMSM used in this paper are shown in table II.

TABLE II. Motor parameters				
Parameter	Value			
Pole pair	4			
Rated speed	3000rpm			
Stator resistance	0.95Ω			
Stator inductance	8.5 <i>mH</i>			
Rotor inertia	$0.003kg \cdot m^2$			
Viscous coefcient	0.0008			
Fux linkage	0.182 <i>Wb</i>			

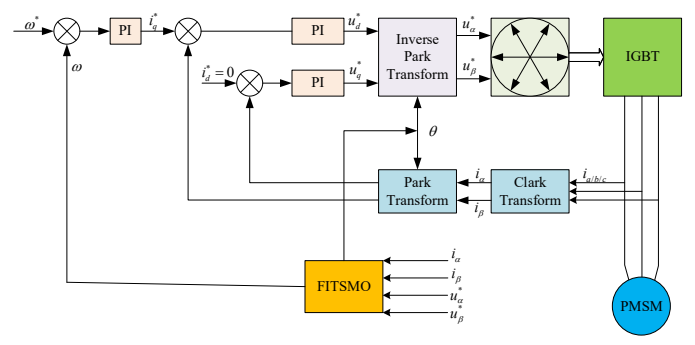
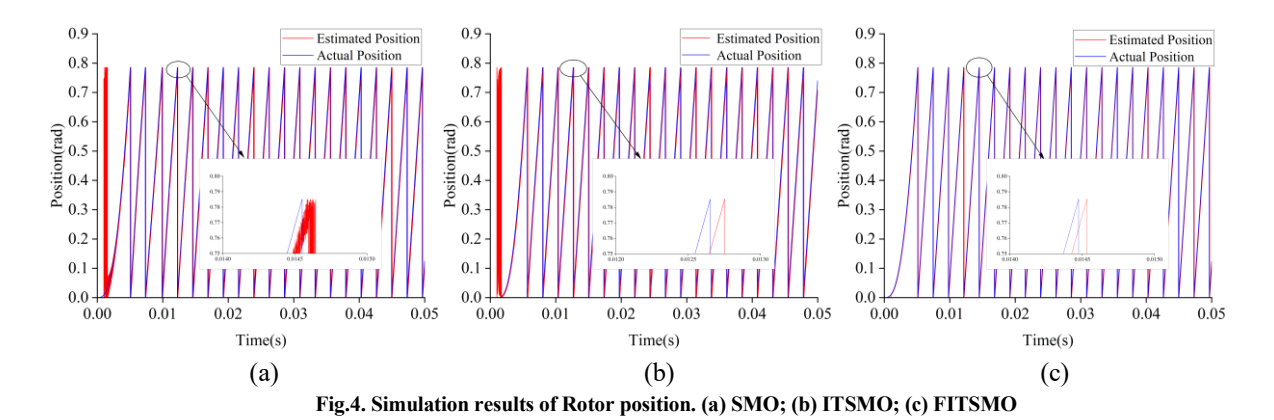


Fig.3 Block diagram of FITSMO

A. Simulation analysis

Based on the block diagram of the PMSM sensorless control system shown in Fig.3, a corresponding simulation model is built in Simulink software. The motor starts with no load initially, and the set rotational speed is 800 rpm. When the motor has been running for 0.1 s, the system rotational speed suddenly changes to 1000 rpm. When the motor has been running for 0.2 s, a load disturbance of $5N \cdot \text{m}$ load torque is applied. The simulation waveforms of the SMO, ITSMO and FITSMO systems are shown in Fig.4 to Fig.6.



As Fig.4 shows, compared with the SMO control, the ITSMO control improves the accuracy of the system's rotor position estimation. As shown in Fig.4 (c), by introducing FLC into the ITSMO, the FITSMO provides a more accurate rotor position estimation than the ITSMO and exhibits better system control performance.

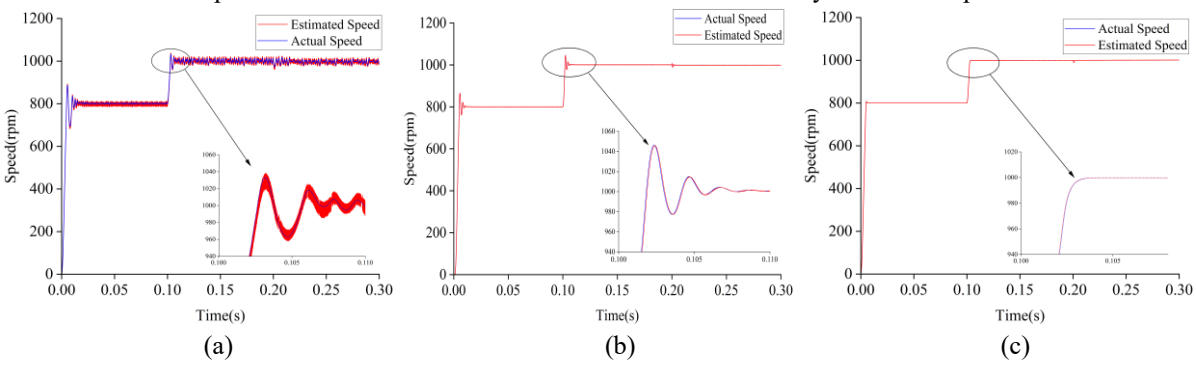
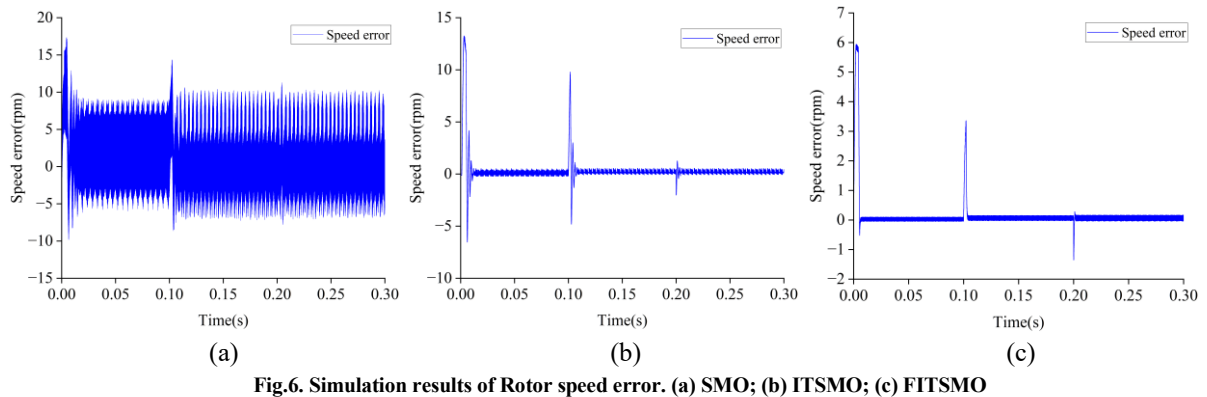


Fig.5. Simulation results of Rotor speed. (a) SMO; (b) ITSMO; (c) FITSMO

We can see from Fig.5, regardless of whether the controlled motor speed is at 800 rpm or 1000 rpm, the system can reach the given value with a relatively fast response speed, but there is still a certain overshoot. The traditional SMO control has a relatively large speed overshoot. Compared with the traditional SMO control, the ITSMO control has a smaller speed overshoot and provides a more accurate speed estimation. As shown in Fig.5 (c), by introducing FLC into the ITSMO, it can be seen that the FITSMO has an even smaller speed overshoot compared to the ITSMO system, weakens the system chattering, and achieves a more accurate speed estimation.



There is a certain error between the predicted speed and the actual speed of the motor. As can be seen from Fig.6 (a)-(b), the estimation of the rotor speed by the SMO has relatively large fluctuations, with the speed error ranging from -10 to 10 rpm. In contrast, the speed estimation error of the ITSMO is between -0.2 and 0.5 rpm. According to Fig.6 (c), the difference between the estimated value of the rotor speed by the FITSMO and the actual speed is within the range of -0.05 to 0.1 rpm. The FITSMO control system has smaller speed fluctuations, stronger anti-interference ability, and higher estimation accuracy. In comparison with the obvious chattering in the speed error of the SMO, the FITSMO designed in this paper significantly suppresses chattering, and the entire control system demonstrates strong robustness.

B. Experimental verification

To verify the feasibility and effectiveness of the control strategy designed in this paper, a PMSM speed regulation system experimental platform shown in Fig.7 is built. The control core of the experimental platform adopts an STM32F407 chip. The PMSM used is DMKE-60BM-01330C5-C, with a rated speed of 3000 rpm and a rated power of 0.4 kW. The PC host computer is used to burn the program into the controller, the hysteresis brake is used to apply load to the motor, the adjustable power supply is used to adjust the load magnitude applied by the hysteresis brake, and the relevant experimental data are transmitted to the PC host computer through the serial port.

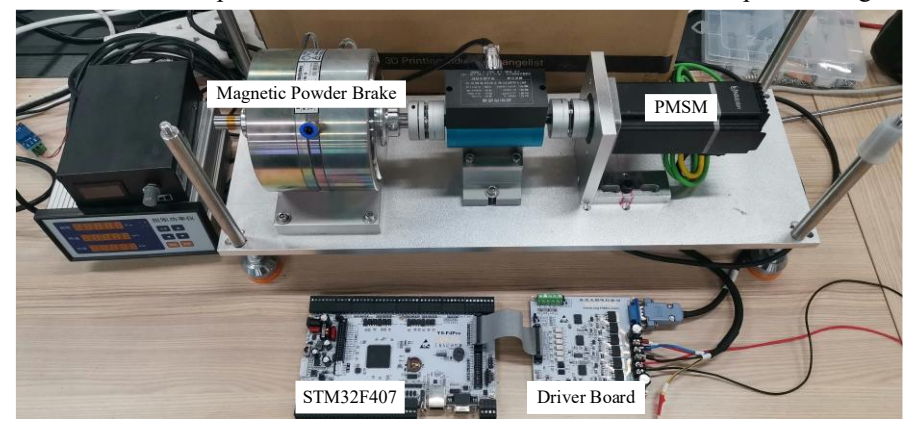


Fig.7. Motor experimental platform

The experimental waveforms of the control speed for SMO, ITSMO, and FITSMO are shown in Fig.8. Table III shows the comparison of the experimental results of the three control methods. From Fig.8 (a), when the system given speed is 1000 rpm, the SMO control has large chattering, which affects the operating performance of the system.

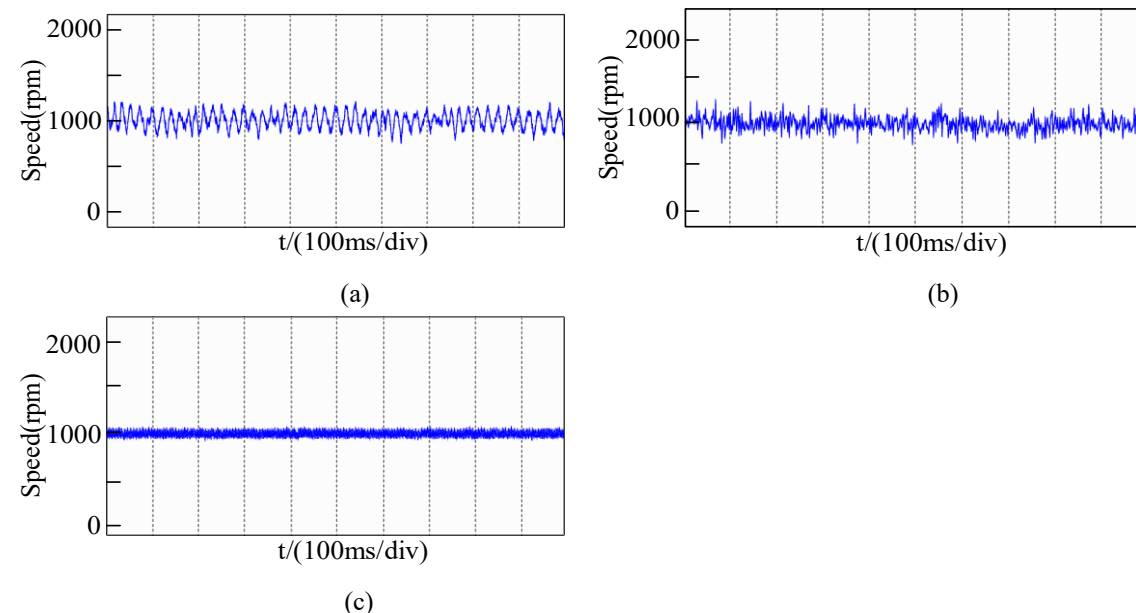


Fig.8. Experimental results of Rotor speed. (a) SMO; (b) ITSMO; (c) FITSMO

	TABLE III. Experimental results				
	SMO	ITSMO	FITSMO		
Speed error	18rpm	1.4rpm	0.3rpm		

As can be seen from Fig.8, compared with the SMO control, the ITSMO significantly weakens the system chattering and improves system stability. The FITSMO control exhibits even smaller chattering and stronger system stability than the ITSMO control. When sudden load addition or removal occurs, the system has the advantage of shorter stabilization time.

The back EMF waveforms of the SMO, ITSMO, and FITSMO control systems are shown in Fig.9. As can be seen from Fig.9 (a)-(b), compared with the SMO control, the back EMF waveform of the ITSMO control is

smoother, which improves the system control accuracy. As shown in Fig.9 (c), by introducing the FLC into the ITSMO control, the FITSMO has higher control accuracy and better system stability compared with the ITSMO.

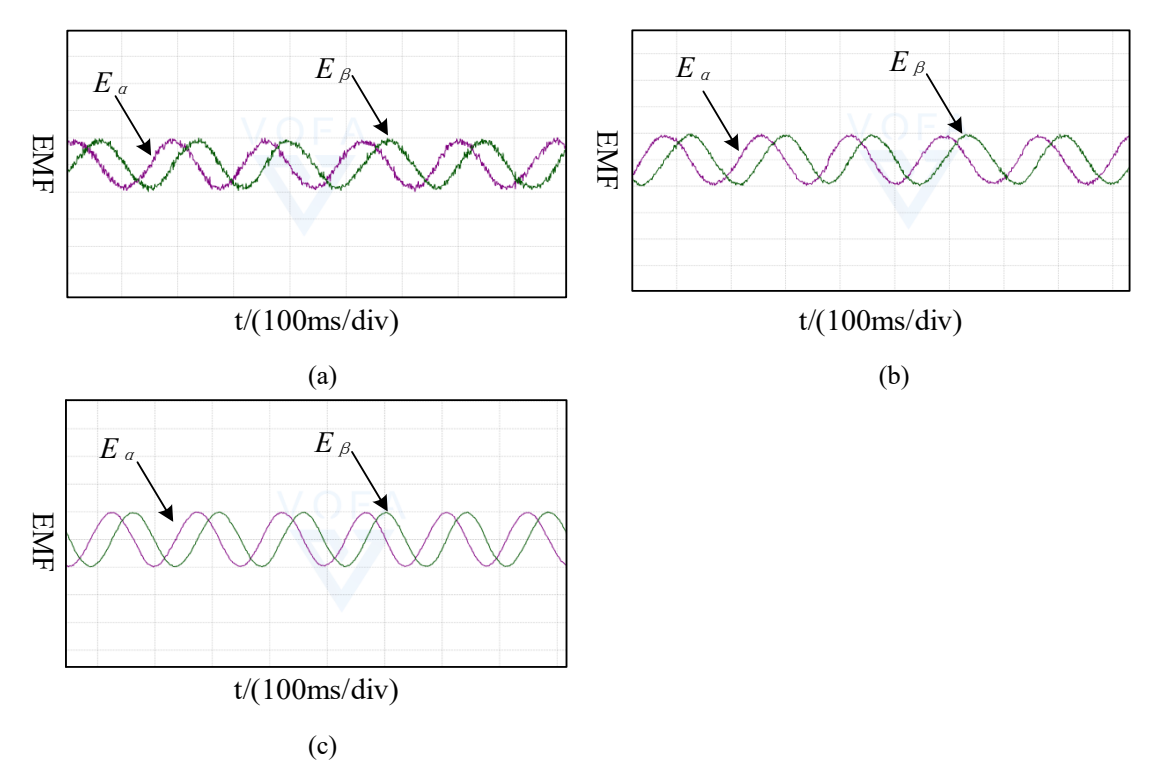


Fig.9. Experimental results of Back EMF. (a) SMO; (b) ITSMO; (c) FITSMO

The FITSMO control proposed in this paper effectively weakens the system chattering, reduces speed fluctuations, improves the accuracy of rotor position estimation, enables the system to stabilize in a shorter time, and enhances system stability compared with the SMO control.

VI. CONCLUSION

This paper proposes a FITSMO control scheme, which introduces FLC into ITSMO control. The fuzzy rules are set with the distance of system dynamic variables approaching the dynamic surface and the dynamic change of the driving speed as rule elements, so as to dynamically and intelligently adjust the driving speed of state variables. This makes the approaching speed of state variables change dynamically with the distance from the sliding surface, improving the stability advantage of the system.

Simulations and experiments show that the FITSMO control significantly improves the system stability. According to the simulation data, the rotor position estimation error of the FITSMO system is approximately 5×10^{-4} rad, and the speed estimation error is within the range of -0.05 to 0.1 rpm. Compared with the SMO control, it has better advantages in chattering control, and the accuracy of the obtained rotor position data and system stability are more prominently demonstrated.

REFERENCES

- [1] Ronggang N, Dianguo X, Frede B, Kaiyuan L, Gaolin W, Guoqiang Z, et al. Square-Wave Voltage Injection Algorithm for PMSM Position Sensorless Control with High Robustness to Voltage Errors[J], IEEE Transactions on Power Electronics, 2017, 32(7): 5425-5437.
- [2] P. L. Xu, Z. Q. Zhu. Novel Carrier Signal Injection Method Using Zero-Sequence Voltage for Sensorless Control of Pmsm Drives[J], IEEE Transactions on Industrial Electronics, 2016, 63(12): 7444-7454.
- [3] Guillermo B, Cristian D A, Jorge S, Guillermo G, et al. Sensorless Pmsm Drive with Tolerance to Current Sensor Faults[C], Conference of the Industrial Electronics Society, 2008: 1326-+.
- [4] Chao G, Yihua H, Guipeng C, Huiqing W, Zheng W, Kai N, et al. A DC-Bus Capacitor Discharge Strategy for PMSM Drive System with Large Inertia and Small System Safe Current in EVs[J], IEEE Transactions on Industrial Informatics, 2019, 15(8): 4709-4718.
- [5] Jiadong L, Xiaokang Z, Yihua H, Jinglin L, Chun G, Zheng W, et al. Independent Phase Current Reconstruction Strategy for IPMSM Sensorless Control Without Using Null Switching States[J], IEEE Transactions on Industrial Electronics, 2018, 65(6): 4492-4502.

- [6] Jinglin L, Chao G, Zexiu H, Haozheng Y, et al. IPMSM Model Predictive Control in Flux-Weakening Operation Using an Improved Algorithm[J], IEEE Transactions on Industrial Electronics, 2018, 65(12): 9378-9387.
- [7] Gaolin Wang, Maria Valla, Jorge Solsona. Position Sensorless Permanent Magnet Synchronous Machine Drives—A Re-view[J], IEEE Transactions on Industrial Electronics, 2019, 67(7): 5830-5842.
- [8] PAN Feng, QIN Guofeng, WANG Chunbiao, et al. Model prediction of MRAS speed sensorless control of PMSM for electric vehicles[J]. Electric Machines&Control Application, 2019, 46(10):104.
- [9] WU Chun, CHEN Ke, NAN Yurong, et al. Variable angle square wave voltage injection for sensorless control of PMSM considering cross saturation effect[J]. Transactions of China Electrotechnical Society, 2020, 35(22):4678.
- [10] Shuaichen Ye, Xiaoxian Yao. An Enhanced SMO-Based Permanent-Magnet Synchronous Machine Sensorless Drive Scheme with Current Measurement Error Compensation[J], IEEE Journal of Emerging and Selected Topics in Power Electronics, 2021, 9(4): 4407-4419.
- [11] ZHOU Juan, SUN Xiao, LIU Kai, et al. Research on SOC estimation algorithm of sliding mode observer with joint extended Kalman filter[J]. Proceedings of the CSEE, 2021,41(2): 692.
- [12] Nanyang Explosion Protected Electrical Apparatus Research Institute, Fan Le, Zhang Zan. Sensorless PMSM Control with Sliding Mode Observer Based on Sigmoid Function[J], Journal of Electrical Engineering and Technology, 2021, 16(2): 933-939.
- [13] Jun-wen MU, Zhong-gen WANG, Wenyan NIE. Integral Terminal Sliding Mode PMSM Sensorless Control Optimiza-tion[J], Power Electronics, 2020, 54(6): 26-29,57.
- [14] TANG J, ZHOU H, ZHANG Z, ZHAO Q, et al. Permanent Magnet Synchronous Motor Sensorless Control Strategy with Super-twisting Sliding Mode Observer[J], Journal of Detection & Control, 2023, 45(2).
- [15] Zebin Y, Dan Z, Xiaodong S, Xiaoting Y, et al. Adaptive Exponential Sliding Mode Control for a Bearingless Induction Motor Based on a Disturbance Observer[J], IEEE Access, 2018, 6: 35425-35434.
- [16] Shihua L, Jun Y, Wen-Hua C, Xisong C, et al. Sliding-Mode Control for Systems with Mismatched Uncertainties Via a Disturbance Observer. [C], Conference of the Industrial Electronics Society, 2012, 60(1): 160-169.
- [17] Yong-peng S, An-kang L, Guang-zhao C, Xiao-liang Y, Zhu-feng Z, et al. Sensorless filed oriented control of per-manent magnet synchronous motor based on extend sliding mode observer[J], Electric Machines and Control, 2020, 24(8): 51-57,66.
- [18] Zhaoping D, Kai L, Yuliang Z, Haifeng W, Guoqiang L, Youquan Z, et al. Permanent Magnet Synchronous Motor Control System Based on a Novel Sliding Mode Observer of Saturation Function[J], Electric Machines & Control Application, 2018, 45(6): 6-11.
- [19] Yurong Nan, Zhanpeng Xing, Jianglong Cheng, Chun Wu, et al. A sliding mode observer for asynchronous motors based on a variable rate reaching law[J], Chinese High Technology Letters, 2021: 969-977.
- [20] Caixia TAO, Kaixuan ZHAO, Qing NIU. Fuzzy super-spiral sliding mode observer for permanent magnet synchronous motor considering sliding mode buffeting[J], Power System Protection and Control, 2019, 47(23): 11-18.
- [21] Huilong Z, Qian Z, Qinhong Z, Qinfeng H, et al. Application of Fuzzy and Sliding Mode Variable Structure Control in Permanent Magnet Synchronous Motor[J], Micromotors, 2018, 51(8): 44-48.